15th Triennial World Congress, Barcelona, Spain

TRANSFER CONTROL AND CURVED PATH DESIGN FOR CYLINDRICAL LIQUID CONTAINER

Masafumi HAMAGUCHI and Takao TANIGUCHI

Department of Electronic and Control Systems Engineering, Shimane University,
1060 Nishikawatsu, Matsue, Shimane, 690-8504 Japan
E-mail: hamaguchi@ecs.shimane-u.ac.jp

Abstract: A spherical pendulum-type model was constructed to represent liquid sloshing in a cylindrical container caused by container transfer along a curved path. The model was used to design a curved path and a transfer control system in consideration of the damping of sloshing in the container. The curvature radius of the curved path and the acceleration of the container were determined using an input shaping method. The effectiveness of the present method was clarified through experiment and simulation. *Copyright ©2002 IFAC*

Keywords: Transportation control, Open loop control systems, Industrial production systems, Vibration dampers, Path planning, Velocity control.

1. INTRODUCTION

With the advancement of automation at various factories, liquid container transfers, such as transfers of molten metals, transfers of molds after pouring as part of material processing in steel and casting industries, or transfers of raw material solutions and mixed solutions in chemical plants without the use of pipes, have become very important processes in production line. In liquid container transfers, sloshing (liquid vibration) is generated by changes in the container's acceleration. Overflows and degradation of quality caused by sloshing in containers are problems that directly affect productivity.

We reported a transfer control system involving a rectangular container on a straight path (Hamaguchi and Terashima, 1994; Yano, et al., 1996). In actual processes, transfer paths often include curved sections, and cylindrical containers are also usually used. In a curved path transfer using a cylindrical container, a swirling phenomenon or rotary sloshing is sometimes observed. Therefore, we developed a model of sloshing and a two-degree-of-freedom control system in a cylindrical container transfer along a curved path (Hamaguchi, et al., 1997). By using only the container velocity control, however, the lateral sloshing was not damped.

This paper describes a transfer control system employing a path design that completely damps the sloshing in a cylindrical container. The usefulness of the present method is demonstrated by means of simulations and experiments.

2. EXPERIMENTAL APPARATUS

A schematic drawing of the experimental apparatus is shown in Figure 1. An automotive cart with a driving wheel horizontally transports a cylindrical container along a transfer path. The driving wheel is driven by an AC servomotor through a timing belt. The radius of the container is 0.1 m, its height is 0.42

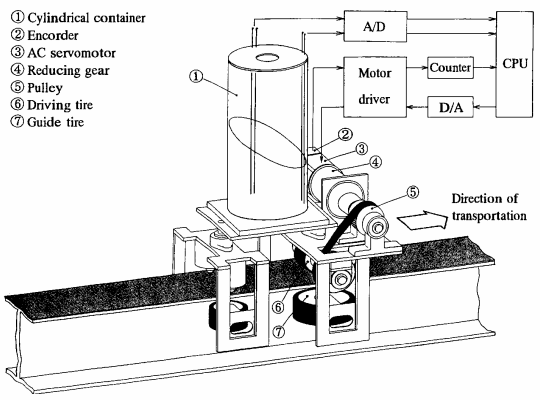

Fig. 1 Schematic drawing of experimental apparatus

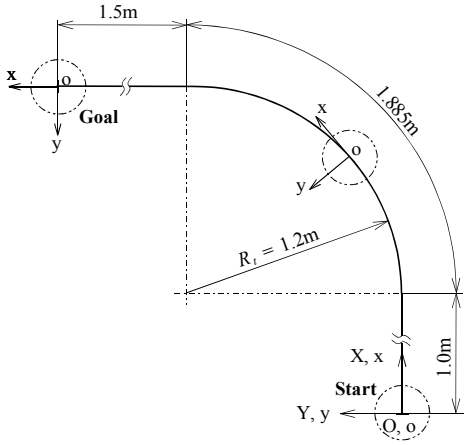

Fig. 2 Transfer path

m, and the liquid level is 0.2 m. Water is chosen as the target liquid because of its simplicity of handling and low cost.

The velocity of the container is controlled by the input voltage to the AC servomotor. The container position is measured by a rotary encoder installed in the AC servomotor. Two sensors are used to observe the liquid level in the front wall and the left side wall. These sensors detect the displacement of the liquid level as a change of the electrical resistance between two electrodes made of stainless steel.

Figure 2 shows the transfer path that consists of three sections: a straight path of 1.0 m, a quarter of a circular arc of 1.2 m radius, and a straight path of 1.5 m. The total transfer length is 4.385 m.

3. MODELS OF LIQUID CONTAINER AND TRANSFER SYSTEM

The spherical pendulum-type sloshing model (Hamaguchi, et al., 1997) is shown in Figure 3. The sloshing model approximately expresses (1, 1)-mode sloshing (Sudo and Hashimoto, 1986), which is a dominant mode of sloshing in the case of container transfer. In this model, the liquid surface is considered to be the plane perpendicularly installed on the pendulum. That is to say, the sloshing has been replaced with the motion of the pendulum. The equations of the sloshing model are as follows:

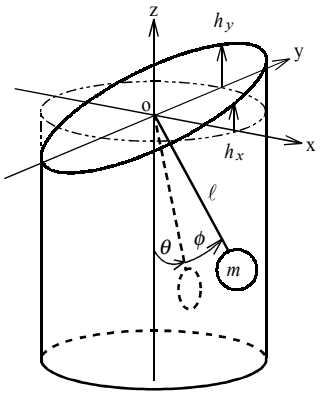

Fig. 3 Spherical pendulum-type sloshing model

$$
\begin{cases}
\ddot{\theta} &= -\dfrac{g\sin\theta}{\ell\cos\phi} + 2\dot{\theta}\dot{\phi}\tan\phi + 2\dot{\phi}\dfrac{\dot{x}_p}{R_t}\cos\theta \\
&\quad + \dfrac{\dot{x}_p^2}{R_t^2}\sin\theta\cos\theta - \dfrac{c_\theta}{m}\dot{\theta}\cos^2\theta \\
&\quad + \dfrac{c_\theta}{m}\dot{\phi}\sin\theta\cos\theta\tan\phi \\
&\quad + \ddot{x}_p\cos\theta\left(\dfrac{\tan\phi}{R_t} - \dfrac{1}{\ell\cos\phi}\right) \\
\ddot{\phi} &= -\dfrac{g\sin\phi}{\ell\cos\theta} + 2\dot{\theta}\dot{\phi}\tan\theta\sin^2\phi \\
&\quad - 2\dot{\theta}\dfrac{\dot{x}_p}{R_t}\cos\theta\cos^2\phi - \dfrac{\dot{x}_p^2}{\ell R_t}\cos\phi \\
&\quad + 2\dot{\phi}\dfrac{\dot{x}_p}{R_t}\sin\theta\sin\phi\cos\phi \\
&\quad + \left(\dfrac{\dot{x}_p^2}{R_t^2} - \dot{\theta}^2\right)\sin\phi\cos\phi \\
&\quad - \dfrac{c_\phi}{m}\dot{\phi}\cos^2\phi - \dfrac{\ddot{x}_p}{R_t}\sin\theta\cos^2\phi \\
&\quad - \ddot{\theta}\tan\theta\sin\phi\cos\phi
\end{cases}
\tag{1}
$$

where θ is the angle of the pendulum mapped onto the z-x plane, ϕ is the angle between the original pendulum and the mapped pendulum, g is the gravitational acceleration, ℓ is the equivalent length of the pendulum, x_p is the position of the container along the transfer path, R_t is the radius of the curved path, m is the mass of the liquid, and c_θ and c_ϕ are the equivalent coefficients of viscosity for sloshing on θ and ϕ, respectively. The displacement of the liquid level at the front wall of h_x and that at the left side wall of h_y are described as

$$
h_x = R\tan\theta, \quad h_y = R\tan\phi/\cos\theta \tag{2}
$$

where R is the inside radius of the cylindrical container.

Equations (1) and (2) are linearized by using a linear approximation technique in order to create a linear control system, because the above nonlinear model is too complicated to allow for the design of a control system. The linearized equations are as follows:

$$
\ddot{\theta} = -\frac{g}{\ell}\theta - \frac{c_\theta}{m}\dot{\theta} - \frac{1}{\ell}\ddot{x}_p, \quad h_x = R\theta \tag{3}
$$

$$
\ddot{\phi} = -\frac{g}{\ell}\phi - \frac{c_\phi}{m}\dot{\phi} - \frac{1}{\ell}a_\phi, \quad h_y = R\phi \tag{4}
$$

where a_ϕ is the centripetal acceleration of $\dot{x}_p^2/r$, and r is the radius of curvature of the curved path. The nonlinear term a_ϕ is not omitted, because that is the main external force on ϕ Equation (3) is used for the design of the transfer control system, and Eq. (4) is employed in the design of the curved transfer path.

In AC servomotors, transfer functions from input voltages to rotational speeds are approximated by

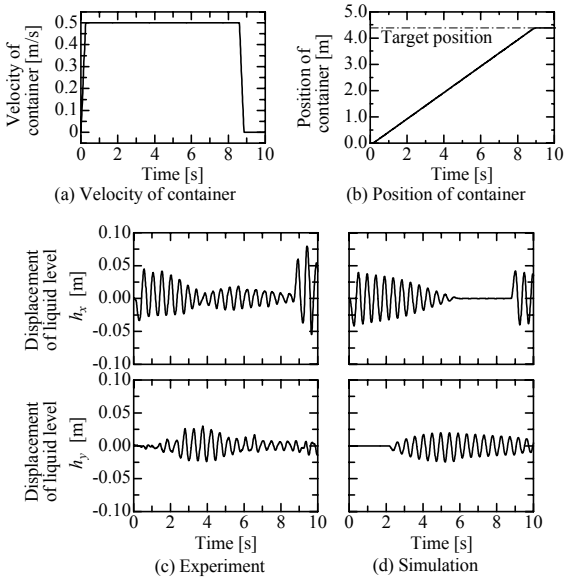

Fig. 4 Validity of sloshing model in transfer state

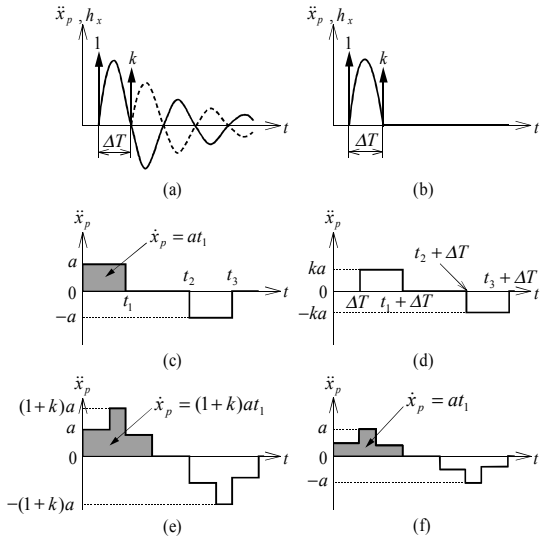

Fig. 5 Transfer control using input shaping method to reduce sloshing

first-order systems. Therefore, the transfer system is described by the following model equation.

$$\ddot{x}_p = -\frac{\dot{x}_p}{T_m} + \frac{K_m}{T_m} u \tag{5}$$

where T_m and K_m are the time constant and the gain, respectively, and u is the input voltage as the control input.

Values of the model parameters in our experimental apparatus are as follows: ℓ = 0.0544 m, m = 6.28 kg, $c_\theta = c_\phi$ = 1.4 Ns/m, R_t = 1.2 m, T_m = 0.0149 s, K_m = 0.0992 m/(sV).

Figure 4 shows a comparison between simulation results and experimental results, where the container is transported using a trapezoidal velocity pattern, namely, a maximum acceleration of 2.0 m/s^2, a uniform velocity of 0.5 m/s, and a deceleration of –2.0 m/s^2. Figure 4(d) shows the simulation results for the nonlinear sloshing model of Eq. (1) calculated using the Runge Kutta method in 0.001 s sampling time. The characteristic behavior of the experimental values and the simulation values agrees closely, as seen in Figures 4(c) and (d).

4. TRANSFER CONTROL

The transfer control system is constructed as an open loop control system without employing sensor feedback to monitor sloshing. The open loop control system is excellent from the viewpoint of cost, when modeling errors and disturbances can be neglected. Many sensors and high-performance computers are required in feedback control systems. In actual transfer systems, fixed transfer control inputs can be easily utilized.

4.1 Input Shaping Method

An input shaping method (Singer and Seering, 1990) is adopted for the transfer control system. The principle of the two-impulse input technique is illustrated in Figures 5(a) and (b). The vibration caused by the unit impulse input of the acceleration is canceled by another impulse input that has an amplitude of k and a time delay of ΔT. When the transfer function from the acceleration of the container to the displacement of the liquid level is a linear second-order system as shown in Eq. (6), ΔT and k can be formulated as Eqs. (7) analytically (Singer and Seering, 1990).

$$\frac{h_x}{\ddot{x}_p} = \frac{-\frac{R}{\ell}}{s^2 + \frac{c_\theta}{m}s + \frac{g}{\ell}} = \frac{K\omega_n^2}{s^2 + 2\zeta\omega_n s + \omega_n^2} \tag{6}$$

$$\Delta T = \frac{\pi}{\omega_n\sqrt{1-\zeta^2}}, \quad k = \exp\left(\frac{-\zeta\pi}{\sqrt{1-\zeta^2}}\right) \tag{7}$$

Equation (6) is derived from Eqs. (3) and (5), where ω_n is the system's natural frequency and ζ is the system's damping ratio.

Figure 5(c) shows the acceleration pattern for the trapezoidal velocity one, where a is the maximum acceleration, t_1 is the acceleration time, at_1 denotes the maximum velocity, t_2 is the end time of uniform velocity or the start time of deceleration, and t_3=t_1+t_2 is the transfer finish time. This acceleration is the input of the minimum time transfer on equipment performance, and it is considered the input without the control. In our experimental apparatus, a=2.0 m/s^2, t_1=0.25 s, t_2=8.77 s, and t_3=9.02 s. Figures 5(d) – (f) illustrate the input shaping method applied to liquid container transfer. The acceleration pattern in

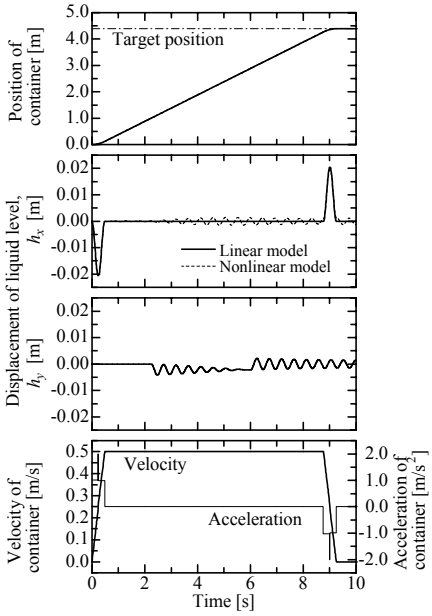

Fig. 6 Simulation results of transfer control using input shaping method

Figure 5(d) cancels the displacement of liquid level h_x generated by the acceleration described in Figure 5(c). Figure 5(e) shows the acceleration to cancel residual vibrations, in which the acceleration pattern is obtained by combining Figure 5(c) with Figure 5(d). However, the transfer velocity $(1+k)at_1$ indicated by the shaded area increases from the maximum velocity at_1 because k is the positive value, as shown in Eq. (7). By using this acceleration pattern, the container should pass the target position. Figure 5(f) shows the transfer acceleration pattern obtained by dividing $1+k$ into one in Figure 5(e). This operation enables the container to arrive at its target position.

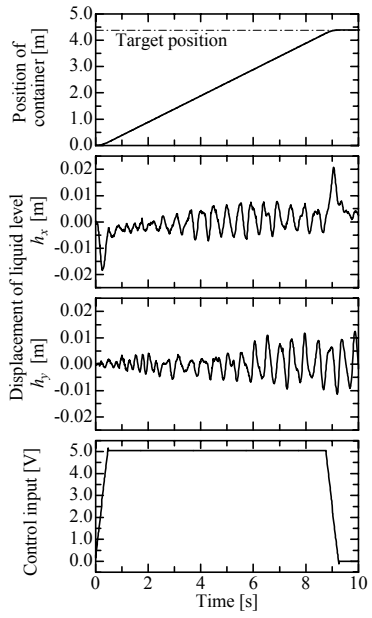

Fig. 7 Experimental results of transfer control using input shaping method

4.2 Results of Simulations and Experiments

Figure 6 shows simulation results of the transfer control using the input shaping method, where ΔT= 0.234 s and k=0.974. The acceleration pattern obtained by the present method is applied to the linear sloshing model and nonlinear model using the Runge Kutta method with 0.001 s sampling time. With respect to h_x, there is no residual vibration at the endpoint of acceleration or deceleration in the linear model. In the nonlinear model, a sufficient damping effect is clearly demonstrated by comparison with non-control results in Figure 4(d). The maximum velocity of the container is 0.5 m/s and the target position of 4.385 m is achieved.

Experimental results of the transfer control are shown in Figure 7. The control input is calculated from Eq. (5) in order to realize the acceleration of Figure 6. This can be considered a good result by comparison with the non-control results shown in Figure 4(c).

5. DESIGN OF CURVED PATH

In the present linear controller, it is impossible to control the displacement of the liquid level h_y directly. The displacement h_y is not controllable in a linear control theory, as it is made clear by Eqs. (4) and (5). In order to damp the displacement h_y, the radius of curvature of the curved path should be designed by using the input shaping method. The usefulness of transfer control on the designed path is demonstrated by the simulation results.

In the transfer control shown in Figure 6, the container moves on the curved path between 2.2 s and 6.1 s, where the velocity of the container $\dot{x}_p$ is the constant value of v=0.5 m/s. In the transfer control on a non-designed path shown in Figure 2, the acceleration a_ϕ in Eq. (4) becomes the constant value of $\dot{x}_p^2 / R_t$ on the curved path, and it becomes the zero on the straight path. That is to say, the shape of the acceleration a_ϕ is correspondent to that of the acceleration a shaded in Figure 5(c). The value of acceleration a_ϕ $(=\dot{x}_p^2 / r)$ is changed according to the radius of curvature of the curved path r because the velocity of the container $\dot{x}_p$ is the constant value of v.

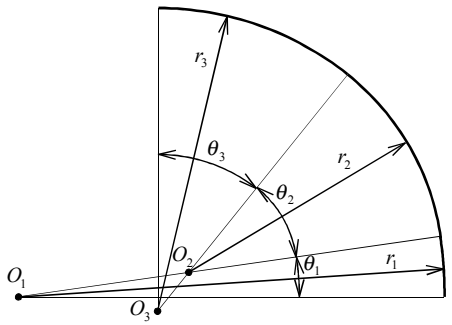

Fig. 8 Designed curved path

The acceleration a_ϕ in the input shaping method is realized using a curved path composed of three sections with different curvature radii shown in Figure 8. It is proven that h_x, $\ddot{x}_p$, and c_θ in Eq. (6) correspond to h_y, a_ϕ, and c_ϕ in Eq. (4), respectively. The parameters ΔT and k in the input shaping method are given by Eqs. (7), and values of ΔT and k are identical with values in the transfer control. In each section, the radius of curvature and the central angle are as follows:

$$r_1 = \frac{v^2}{\alpha_{y1}} = (1+k)R_t, \quad \theta_1 = \frac{v\Delta T}{r_1} \tag{8}$$

$$r_2 = \frac{v^2}{\alpha_{y2}} = R_t, \quad \theta_2 = \frac{v(t_1 - \Delta T)}{r_2} \tag{9}$$

$$r_3 = \frac{v^2}{\alpha_{y3}} = \frac{(1+k)}{k} R_t, \quad \theta_3 = \frac{v\Delta T}{r_3} \tag{10}$$

where t_1 is the running time on the non-designed curved path. Denoting the desired central angle as θ_d, the value of t_1 is described with $\theta_d R_t / v$. Those centers of rotation are the points of O_1, O_2, and O_3, where the next center of rotation is placed on the radius line in the endpoint of the former section for the sake of a smooth connection. In our experimental apparatus, R_t = 1.2 m, v = 0.5 m/s, and $\theta_d = \pi/2$ rad. It is possible to easily confirm $\theta_1 + \theta_2 + \theta_3 = \theta_d$ from Eqs. (8), (9), and (10). The designed path of the liquid container transfer is obtained to thus replace the curved path in Figure 2 with that of Figure 8.

Figure 9 shows the simulation results of the transfer control applied in the nonlinear sloshing model. By comparison with results of the transfer control using the non-designed path of Figure 2, the effectiveness of the present design method for the curved path becomes obvious from the viewpoint of damping not only the displacement of the liquid level of h_y but also that of h_x. However, the position of the container exceeds the target position by $v\Delta T$=0.117 m, and the transfer finish time is lengthened by ΔT=0.234 s. The differences between the goal point of the designed path and that of the non-designed path are 0.059 m on the X-axis and 0.061 m on the Y-axis, respectively. Axes are shown in Figure 2. The adjustment of the designed path is carried out so that the goal position of the designed path may agree with that of the non-designed path. The lengths of the straight sections in the designed path are shortened form 1.0 m to 0.941 m and from 1.5 m to 1.439 m, respectively. Using this adjustment, the difference between the designed path and the non-designed path is slightly 0.003 m in the total transfer length, and both transfer finish times are almost equal.

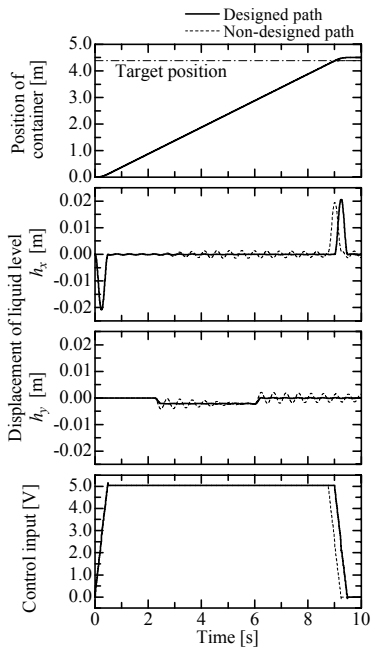

Fig. 9 Simulation results of transfer control on designed path applied in the nonlinear sloshing model

6. EVALUATION OF ROBUSTNESS

The two-impulse input technique of input shaping cancels vibrations perfectly only if both the system's natural frequency ω_n and damping ratio ζ, namely, both the time delay ΔT and the amplitude k, are exact. In order to quantify the damping effect for sloshing, a performance index must be defined in Eq. (11) for a transfer control.

$$J = \int_0^{t_f} \left(|h_x| + |h_y| \right) dt \tag{11}$$

where t_f is the calculation finish time, here, t_f = 12 s. Modeling error and operation input error due to the inaccuracy of the equipment can create a case in which the correct transfer control is not carried out. Namely, this is a case in which the values of the parameters of ΔT and k differ from right values. In order to evaluate the robustness of the control system, the performance index of Eq. (11) is used, where the performance index is calculated using the simulation results of the transfer control of the designed path applied in the nonlinear sloshing model.

Figure 10 shows the degradation of the performance index when ΔT and k are changed from the true value. The values of the performance index are calculated by means of simulation results of the transfer control applied in the nonlinear sloshing model. Symbols α, β, and γ denote the rate of change for ΔT, k, and the degradation rate of the performance index J, respectively. These are defined as follows:

$$\alpha = (\Delta T / \Delta T_r - 1) \times 100 \ [\%] \tag{12}$$

$$\beta = (k / k_r - 1) \times 100 \ [\%] \tag{13}$$

$$\gamma = (J / J_r - 1) \times 100 \ [\%] \tag{14}$$

where ΔT_r and k_r are the true values of ΔT and k for the system, respectively, and J_r is the value of J in

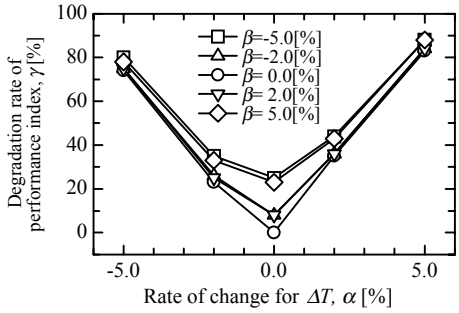

Fig. 10 Degradation rate of performance index as the parameters of the input shaping method are changed

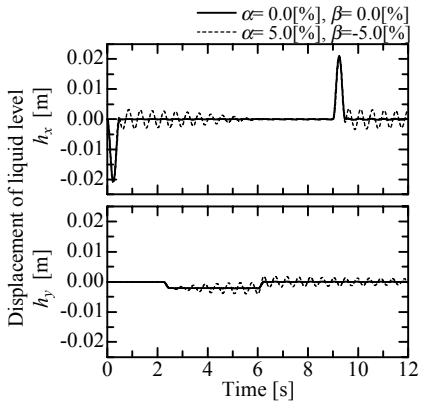

Fig. 11 Simulation results of transfer control as the parameters of the input shaping method are changed

the transfer control using ΔT_r and k_r. The error of the time delay of ΔT deteriorates the performance index of J further than the error of the amplitude of k. This means that the timing of the control input is more important for cancelling the residual vibration.

Simulation results of the worst case in Figure 10 are shown in Figure 11. The maximum amplitudes of the residual vibrations of h_x and h_y are 1.74 % and 0.925 %, which are not too large for a standing liquid level of 0.2 m, respectively. Therefore, the present transfer control system for liquid containers is sufficiently effective.

7. CONCLUSION

In this paper, a simplified model of sloshing has been constructed using a spherical pendulum. The transfer control system and the transfer path have been designed by means of an input shaping method for application in a sloshing model. The control input has been realized by employing a very simple acceleration pattern, and the designed path is very similar to the non-designed path in regard to total transfer length. The robustness of the proposed method has been quantitatively evaluated by a performance index to indicate the damping effect on sloshing. It is notable that the proposed transfer control system can be constructed at a low cost and has a sufficient damping effect to control sloshing. This transfer control system will be highly useful if the present method is applied for transfer systems involving wheeled mobile robots.

REFERENCES

Hamaguchi, M., Yamamoto, M. and Terashima, K. (1997). Modeling and Control of Sloshing with Swirling in a Cylindrical Container during a Curved Path Transfer. *Proc. of the ASCC*, **Vol.1**, 233/236.

Hamaguchi, M., and Terashima, K. (1994). Modeling and Optimal Control of Liquid Vibration in Transferring a Rectangular Container. *Proc. of the FLUCOME*, **Vol.1**, 379/384.

Yano, K., Yoshida, T., Hamaguchi, M. and Terashima K. (1996). Liquid Container Transfer Considering the Suppression of Sloshing for the Change of Liquid Level. *Proc. of the IFAC'96*, **Vol.B**, 193/198.

Sudo, S. and Hashimoto, H. (1986). Dynamic Behavior of a Liquid in a Cylindrical Container Subject to Horizontal Vibration. *Trans. of the Japan Society of Mechanical Engineers (B)*, **Vol.52**, **No.483**, 3655/3659.

Singer, N.C. and Seering, W.P. (1990). Preshaping Command Inputs to Reduce System Vibration. *ASME J. of Dynamic Systems, Measurement, and Control*, **Vol.112**, 76/82.